Lattice effects on the transport properties of $(R,Sr)_3Mn_2O_7$ (R=La, Eu, and Pr)

Sandip Chatterjee, P. H. Chou, C. F. Chang, I. P. Hong, and H. D. Yang
Department of Physics, National Sun Yat-Sen University, Kaohsiung, Taiwan 804, Republic of China
(Received 19 August 1999)

The resistivity, magnetoresistance, and thermoelectric power (TEP) of $R_{1.4}(Sr_{1-y}Ca_y)_{1.6}Mn_2O_7$ and $R(Sr_{1-y}Ca_y)_2Mn_2O_7$ (R=La, Eu, Pr) have been studied to investigate the lattice effects (when the Mn^{4+} concentration is 30 and 50 %) on the transport properties. The semiconducting behavior in the resistivity curve can be explained with the nearest-neighbor small polaron hopping. A changeover from the adiabatic to the nonadiabatic regime in the hopping mechanism is observed when the ratio of $Mn^{4+}/(Mn^{3+}+Mn^{4+})$ changes from 30 to 50 %. The behavior of the magnetoresistance in $R_{1.4}(Sr_{1-y}Ca_y)_{1.6}Mn_2O_7$ is different from that in $R(Sr_{1-y}Ca_y)_2Mn_2O_7$ which might be due to the presence of a more complex magnetic interaction dominated by superexchange in $R(Sr_{1-y}Ca_y)_2Mn_2O_7$. The TEP data below the metal-insulator transition of $R_{1.4}(Sr_{1-y}Ca_y)_{1.6}Mn_2O_7$ are the combinations of the phonon drag and the diffusion thermopower but in $RSr_2Mn_2O_7$ some other terms may be present.

I. INTRODUCTION

The panorama of properties[1–10] exhibited by $R_{1-x}A_xMnO_3$ (where R and A are rare-earth and alkaline-earth elements, respectively), such as colossal magnetoresistance (CMR), metal-insulator transition, charge and magnetic ordering, etc., have generated an impulse in these manganite systems, particularly on the interplay among the structure, magnetism, and electronic transport. Depending on the doping level (x) and temperature, these systems present different phases of conduction and complicated magnetic phase transitions. However, recently, large magnetoresistance has been observed in other crystal structures, namely, the pyrochlore $Tl_2Mn_2O_7$ (Refs. 11 and 12) and layered $(Nd,Sr)_3Mn_2O_7$.[13] The $(R,A)_3Mn_2O_7$ is considered as the $n=2$ member of the family $(R,A)_{n+1}Mn_nO_{3n+1}$, where n is the number of perovskite layers. In this series, the observed magnetoresistance effect is even stronger than in the perovskites but occurs at a lower Curie temperature T_C.[14] The average structure is tetragonal, made of a bilayer perovskite unit in the ab plane of the crystal, separated by a single rock-salt-type R/A-O layer along the c axis giving it a two-dimensional (2D) character.[15] In particular, the Mn-O-Mn bond angle in the $(La,A)_3Mn_2O_7$ system is about 180° and it does not change significantly with internal and external pressure[16,17] in contrast to the $(La,A)MnO_3$ system where the bond angle is in the range 155–170°,[18,19] which plays a crucial role in these perovskite compounds. Moreover, the bond-length variation with external and internal pressure in $(La,A)_3Mn_2O_7$ and $(La,A)MnO_3$ is different.[16,17,20] Therefore the study of lattice effects on the transport and magnetic properties in the $(R,A)_3Mn_2O_7$ system might provide another idea to elucidate the fundamental understanding of the CMR properties.

In this paper, size effects of the interpolated cations are compared by studying $R_{1.4}(Sr_{1-y}Ca_y)_{1.6}Mn_2O_7$ and $R(Sr_{1-y}Ca_y)_2Mn_2O_7$ (with R=La, Eu, and Pr) where $Mn^{4+}/(Mn^{3+}+Mn^{4+})$ is 30 and 50 %, respectively. These correspond to the $R_{1-x}A_xMnO_3$ with most studied $x=0.3$ and 0.5 compounds. Subsequently, the resistivity, magnetoresistance, and thermoelectric power (TEP) measurements were investigated and the special attention was paid on TEP since it is one of the most sensitive experiments which probes the carriers in the system.

II. EXPERIMENTAL DETAILS

$R_{1.4}(Sr_{1-y}Ca_y)_{1.6}Mn_2O_7$ and $R(Sr_{1-y}Ca_y)_2Mn_2O_7$ (R=La, Eu, Pr) polycrystalline samples were prepared by standard solid-state reaction method. Stoichiometric mixtures of high-purity oxides R_2O_3, $SrCO_3$, $CaCO_3$, and MnO_2 were first calcined in air at 900 °C for 12 h, and reground and fired in air at 1200 °C for 12 h. Then, the obtained powder was pressed into pellets and sintered in air at 1400 °C for 24–48 h with intermediate grindings for three times. Powder x-ray-diffraction data were obtained using SIEMENS D5000 diffractometer with Cu $K\alpha$ radiation at room temperature. The lattice parameters of different samples are listed in Table I. Electrical resistivity was measured on samples of rectangular parallelepipeds using standard four-probe technique. Thermoelectric power (S) was measured using the standard dc method with the use of closed cycle cryocooling system. A temperature difference of 1–2 degrees was maintained between the two parallel surfaces of the samples under investigation. To eliminate the effects from the Cu electrodes and reference leads (Cu wires), the absolute thermopower of Cu was subtracted from the measured thermoelectric voltage.

III. RESULTS AND DISCUSSIONS

Figure 1 shows the temperature dependence of the electrical resistivity for $La_{1.4}(Sr_{1-y}Ca_y)_{1.6}Mn_2O_7$ with $y=0$, 0.1, 0.2, and 0.3. Each plot has a maximum resistivity (ρ_m) at a temperature T_m. It is found that in each case ρ_m increases and T_m decreases with the increase of Ca. In the manganite system at high temperatures the lattice becomes distorted around the electrons in the conduction band, and due to the strong electron-phonon interaction, small polarons are formed. Above T_m the thermally activated hopping of these

TABLE I. The values of lattice parameters (a and c), T_m (metal-insulator transition temperature), T_{mr} [the temperature where the magnetoresistance ratio (MR) shows the maximum value], dT_m/dH (the change of T_m with magnetic field), and MR at 2 T magnetic field for the investigated samples.

Sample	a (Å)	c (Å)	T_m (K)	T_{mr} (K) at 2 T	dT_m/dH (K/T)	MR at 2 T
$La_{1.4}Sr_{1.6}Mn_2O_7$	3.871 88(10)	20.1698(8)	108	105	9	63%
$La_{1.4}(Sr_{0.9}Ca_{0.1})_{1.6}Mn_2O_7$	3.861 44(10)	20.1805(8)	96	90	11	80%
$La_{1.4}(Sr_{0.8}Ca_{0.2})_{1.6}Mn_2O_7$	3.864 88(10)	20.0961(8)	78	60	15	87%
$(La_{0.9}Eu_{0.1})_{1.4}Sr_{1.6}Mn_2O_7$	3.867 35(10)	20.1381(7)	80	75	10	90%
$(La_{0.8}Eu_{0.2})_{1.4}Sr_{1.6}Mn_2O_7$	3.863 63(9)	20.1210(7)	70		2.5	
$Pr_{1.4}Sr_{1.6}Mn_2O_7$	3.833 79(19)	20.2598(8)	85	80	2	35%
$LaSr_2Mn_2O_7$	3.871 18(13)	19.9640(9)	162		1.66	
$La(Sr_{0.9}Ca_{0.1})_2Mn_2O_7$			167		4	
$La(Sr_{0.8}Ca_{0.2})_2Mn_2O_7$			175		3	
$PrSr_2Mn_2O_7$	3.851 56(12)	19.9354(8)				
$La_{0.7}Ca_{0.3}MnO_3$[a]			255		5	70%

[a]Data have been taken from Refs. 24 and 25.

polarons plays an important role. We have shown the high-temperature resistivity as $\log(\rho)$ vs $1000/T$ in the inset of Fig. 1. These data can be analyzed with the nearest-neighbor hopping of small polaron. The expression for the resistivity as proposed by Mott[21] can be written as

$$\rho = A \exp(E_\rho / k_B T), \tag{1}$$

where k_B is the Boltzmann constant, A is the resistivity coefficient, and E_ρ is the activation energy. It is found in Fig. 1 that the data fit nicely to the Eq. (1) with a straight line. The activation energies estimated from the slope of the straight line vary from 82 to 101 meV in $La_{1.4}(Sr_{1-y}Ca_y)_{1.6}Mn_2O_7$ system.

The temperature dependence of resistivity of $La(Sr_{1-y}Ca_y)_2Mn_2O_7$ ($y=0$, 0.1, and 0.2) is shown in Fig. 2. In $La(Sr_{1-y}Ca_y)_2Mn_2O_7$ a minimum is observed in the $\rho(T)$ plot around 60 K and an upturn in resistivity is developed at lower temperature. In fact, there is also a minimum and an upturn in $La_{1.4}(Sr_{1-y}Ca_y)_{1.6}Mn_2O_7$ for $y=0.1$ and 0.2 as seen in Fig. 1. This upturn becomes more pronounced as y increases. But the origin of this feature for the two cases may be different. The minimum and upturn in $La(Sr_{1-y}Ca_y)_2Mn_2O_7$ correspond to the formation of charge ordering,[7] whereas in $La_{1.4}(Sr_{1-y}Ca_y)_{1.6}Mn_2O_7$, it may be due to spin canting which will be discussed later. The resistivity data above T_m, which are similar to those of the $La_{1.4}(Sr_{1-y}Ca_y)_{1.6}Mn_2O_7$ systems, can also be analyzed with the nearest-neighbor hopping of small polaron (shown in inset of Fig. 2).[21] The activation energy (E_ρ) estimated to be 85–107 meV for $La(Sr_{1-y}Ca_y)_2Mn_2O_7$. It is worth mentioning that in $La_{1.4}(Sr_{1-y}Ca_y)_{1.6}Mn_2O_7$ as x increases, ρ also increases but T_m decreases, whereas in $La(Sr_{1-y}Ca_y)_2Mn_2O_7$ as x increases, ρ decreases and T_m increases.

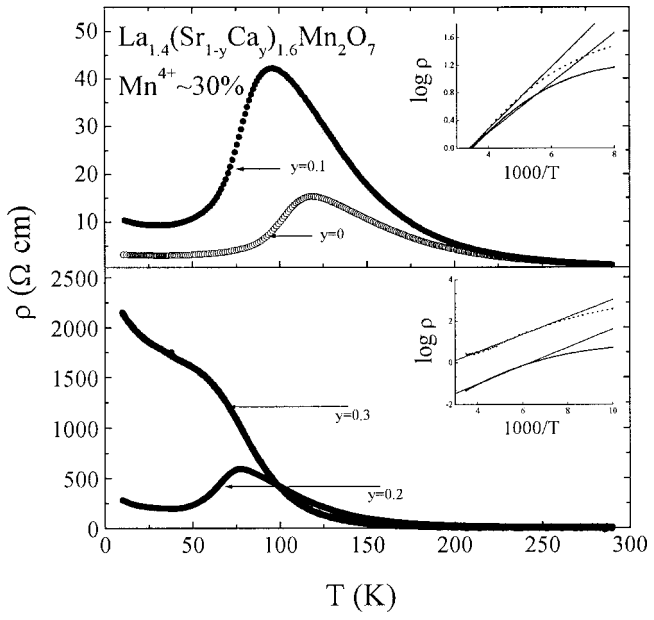

FIG. 1. Temperature variation of resistivity of $La_{1.4}(Sr_{1-y}Ca_y)_{1.6}Mn_2O_7$ with $y=0$, 0.1, 0.2, and 0.3. Insets: Plots of $\log(\rho)$ vs $1000/T$ to show that the conduction above the metal-insulator transition is due to the small polaron hopping.

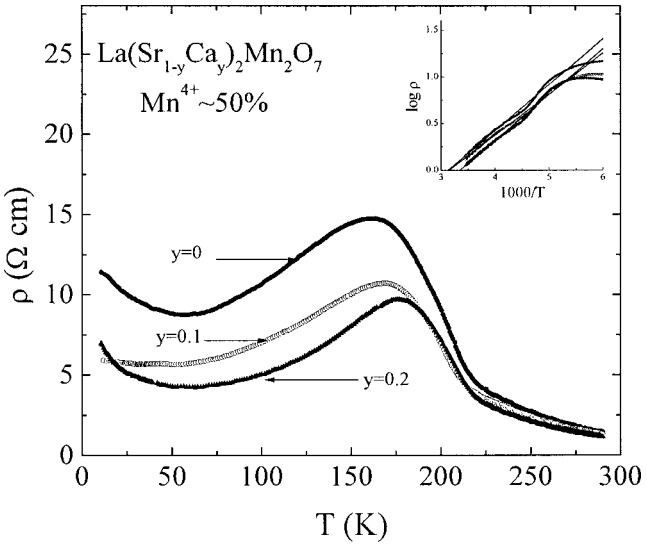

FIG. 2. Temperature variation of resistivity of $La(Sr_{1-y}Ca_y)_2Mn_2O_7$ with $y=0$, 0.1, and 0.2. Insets: Plots of $\log(\rho)$ vs $1000/T$.

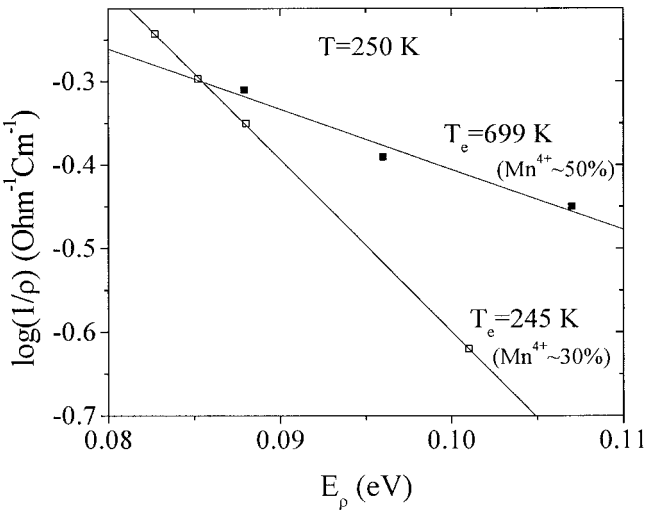

FIG. 3. Plots of $\log(1/\rho)$ vs activation energy (E_ρ) for $La_{1.4}(Sr_{1-y}Ca_y)_{1.6}Mn_2O_7$ (□) and $La(Sr_{1-y}Ca_y)_2Mn_2O_7$ (■) to show that the hopping mechanism is in adiabatic or nonadiabatic regime. T_c is the estimated temperature (discussed in text).

The hopping mechanism (adiabatic or nonadiabatic) of these manganites could be suggested[22] by plotting $\ln(1/\rho)$ vs E_ρ at a fixed temperature. The temperature T_e (say), estimated from the slope of such a plot would be close to the experimental temperature when the hopping is considered to be in the adiabatic regime. On the other hand, T_e would be very different from experimental temperature if the hopping is considered to be in the nonadiabatic regime. Such plots for a fixed temperature ($T=250$ K) for $La_{1.4}(Sr_{1-y}Ca_y)_{1.6}Mn_2O_7$ and $La(Sr_{1-y}Ca_y)_2Mn_2O_7$ are shown in Fig. 3 and the estimated T_e value is 245 K for the former and 650 K for the latter. This implies that the hopping mechanism in $La_{1.4}(Sr_{1-y}Ca_y)_{1.6}Mn_2O_7$ is in the adiabatic regime whereas in $La(Sr_{1-y}Ca_y)_2Mn_2O_7$ is in the nonadiabatic regime. Therefore the hopping mechanism is changing from the adiabatic to the nonadiabatic regime with increasing the Mn^{4+} from 30 to 50%. It has also been shown by Worledge *et al.*[23] that in the $La_{2/3}Ca_{1/3}MnO_3$ thin film, where the concentration of Mn^{4+} is 33%, the conduction in the high-temperature region is governed by the adiabatic small polaron hopping.

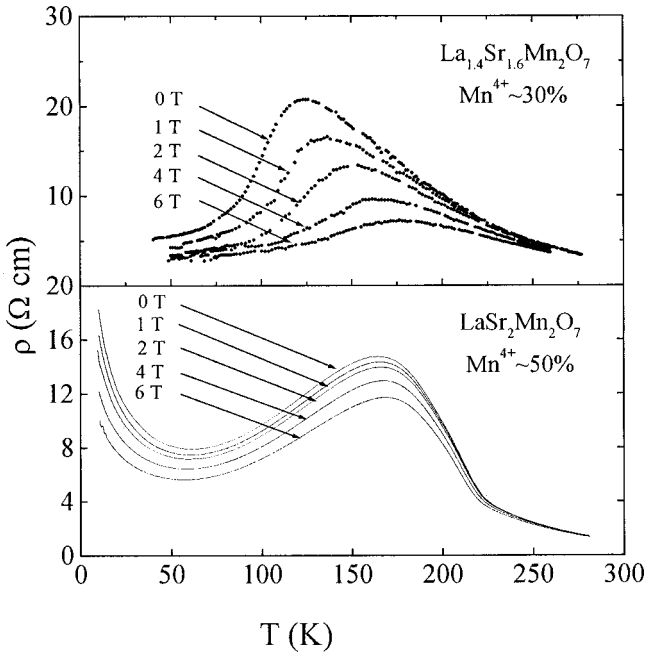

FIG. 4. Temperature variation of resistivity of $La_{1.4}Sr_{1.6}Mn_2O_7$ and $LaSr_2Mn_2O_7$ at different magnetic fields (0–6 T).

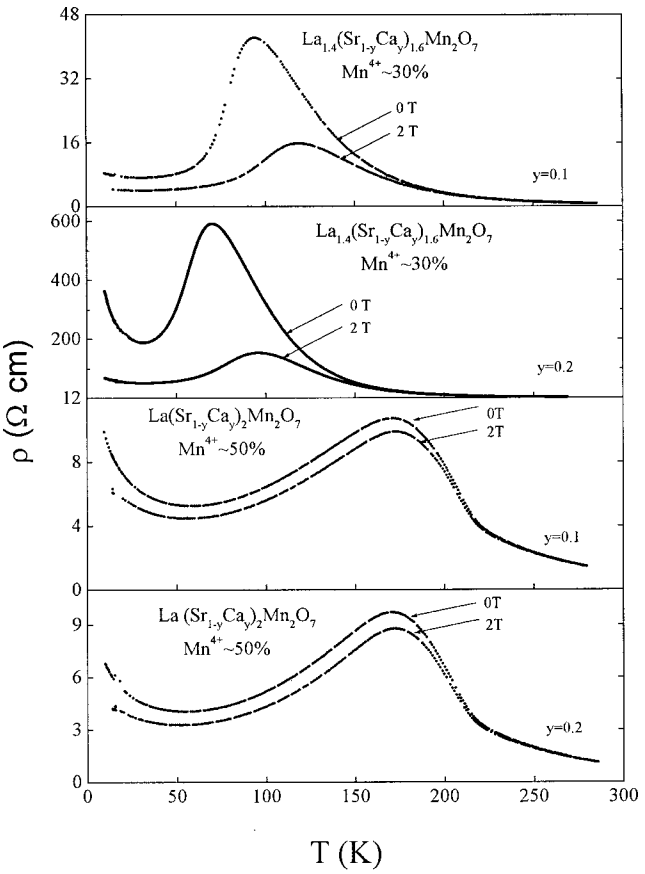

FIG. 5. Temperature variation of resistivity of $La_{1.4}(Sr_{1-y}Ca_y)_{1.6}Mn_2O_7$ and $La(Sr_{1-y}Ca_y)_2Mn_2O_7$ at 0 and 2 T magnetic fields for $y=0.1$ and 0.2.

The magnetic-field effect on the resistivity for $La_{1.4}Sr_{1.6}Mn_2O_7$ and $LaSr_2Mn_2O_7$ is shown in Fig. 4. On applying magnetic field there is a large decrease in the resistivity around the transition temperature and a shift in T_m towards the higher temperature. However, the decrease of ρ_m and the increase of T_m on applying magnetic field is larger in $La_{1.4}Sr_{1.6}Mn_2O_7$ than that in $LaSr_2Mn_2O_7$. Figure 5 presents the temperature dependencies of the resistivity of $La_{1.4}(Sr_{1-y}Ca_y)_{1.6}Mn_2O_7$ ($y=0.1$ and 0.2) and $La(Sr_{1-y}Ca_y)_2Mn_2O_7$ ($y=0.1$ and 0.2) at zero and 2 T magnetic field. For the $La_{1.4}(Sr_{1-y}Ca_y)_{1.6}Mn_2O_7$ with $y=0.2$, the observed upturn at low temperature (around 50 K) is suppressed with applying magnetic field. It may be due to the fact that the disordered spins resulted from the lattice distortion reorient orderly with applying magnetic field which in effect suppress the upturn. The negative magnetoresistance (MR) is higher in $La_{1.4}(Sr_{1-y}Ca_y)_{1.6}Mn_2O_7$ than that in $La(Sr_{1-y}Ca_y)_2Mn_2O_7$. In addition the estimated dT_m/dH of $La_{1.4}(Sr_{1-y}Ca_y)_{1.6}Mn_2O_7$ for $y=0$ is about 9 K/T and increases with increasing y and becomes ~15 K/T for $y=0.2$, which is much larger than that in $La_{1-x}A_xMnO_3$ (~1

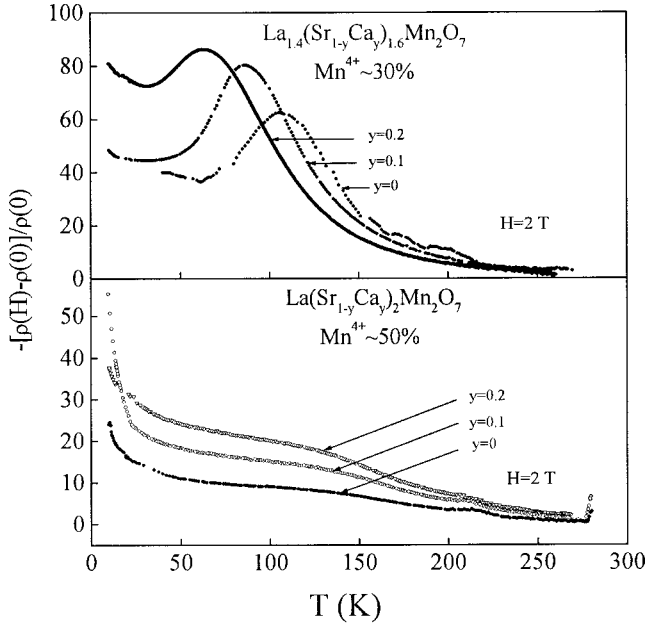

FIG. 6. Temperature variation of magnetoresistance ratio of $La_{1.4}(Sr_{1-y}Ca_y)_{1.6}Mn_2O_7$ and $La(Sr_{1-y}Ca_y)_2Mn_2O_7$ at the magnetic field of 2 T for $y=0$, 0.1, and 0.2.

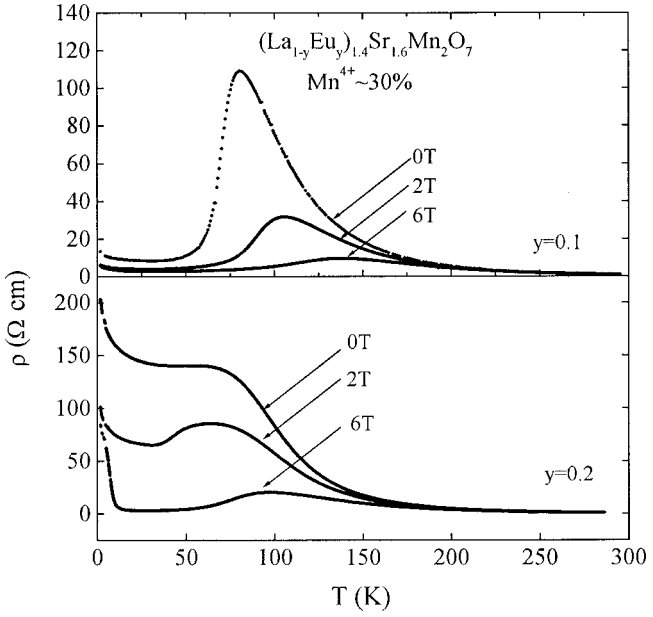

FIG. 7. Temperature variation of resistivity of $(La_{1-y}Eu_y)_{1.4}Sr_{1.6}Mn_2O_7$ with $y=0.1$ and 0.2 under 0, 2, and 6 T magnetic fields.

K/T–6 K/T, $A=$Sr, Ca).[24,25] The dT_m/dH and other parameters for all samples in the present investigation are listed in Table I and compared to those of $La_{1-x}A_xMnO_3$. The negative MR value here is defined as $-[\rho(H)-\rho(0)]/\rho(0)$ [where $\rho(0)$ is the resistivity at zero field and $\rho(H)$ is the resistivity at magnetic field H]. Figure 6 shows the temperature variation of MR of $La_{1.4}(Sr_{1-y}Ca_y)_{1.6}Mn_2O_7$ and $La(Sr_{1-y}Ca_y)_2Mn_2O_7$ with a field of 2 T. In Fig. 6, the MR values of $La_{1.4}(Sr_{1-y}Ca_y)_{1.6}Mn_2O_7$ are 63, 80, and 87% for $y=0$, 0.1, and 0.2, respectively. Similar to the resistivity, the MR ratio data also show a maximum at a temperature T_{mr} which is a little lower than the corresponding metal-insulator transition temperature (T_m). The MR value decreases rapidly as the temperature deviates from the T_{mr}. It is obvious from the above data that the doping of Ca enhances the MR ratio largely in $La_{1.4}(Sr_{1-y}Ca_y)_{1.6}Mn_2O_7$. It seems that the Ca doping in $La_{1.4}(Sr_{1-y}Ca_y)_{1.6}Mn_2O_7$ may induce a chemical pressure which in effect may induce an anisotropic lattice distortion and a canting of ferromagnetic manganese spin configuration and as a consequence, the charge carriers suffer more from scattering by Mn spin which will result in an increase of electrical resistivity. As magnetic field is applied, the canting of the ferromagnetic Mn spins are suppressed and thus electrical resistivity decreases. On the other hand, the MR of $La(Sr_{1-y}Ca_y)_2Mn_2O_7$ (Fig. 6) increases as the temperature decreases and no pronounced peak is found around T_m. The presence of the significantly large MR at low temperature ($T \ll T_m$, where spin fluctuations are negligible) suggests an additional source of magnetoresistance in these samples. The increase of resistivity and low-temperature upturn seen in Fig. 1 can be explained by a ferromagnetic-to-antiferromagnetic transition as Ca content increases. The overlap between the Mn $3d$ orbital and the O $2p$ is the crucial factor in exhibiting electronic conduction[26] which is very sensitive to bond lengths and angles of Mn-O-Mn that result from the variation of the size of the lanthanide ions.[17] This implies the chemical pressure not only affects the magnetic ground states through changing the effective transfer integral in the double-exchange interaction but also the magnetotransport properties by varying the strength of carrier localization effect. Most recently, Argyriou *et al.*[27] and Medarde *et al.*[28] have demonstrated that the temperature dependence of lattice distortion and magnetic structure are dramatically sensitive to the doping level (particularly in the range $0.3 \leqslant x \leqslant 0.4$) in $La_{2-2x}Sr_{1+2x}Mn_2O_7$. Therefore the different MR behavior of $La(Sr_{1-y}Ca_y)_2Mn_2O_7$ ($x=0.5$) from that of $La_{1.4}(Sr_{1-y}Ca_y)_{1.6}Mn_2O_7$ ($x=0.3$) might be due to the presence of a more complex magnetic interaction dominated by superexchange over double exchange.[29] The possible charge ordering of Mn^{3+} and Mn^{4+} in $La(Sr_{1-y}Ca_y)_2Mn_2O_7$ could also lead to electron localization and contribute to the complex nature of this transition.[29] Therefore when Mn^{4+} concentration is increasing from 30 to 50% the localization also increases. In addition, the MR of the $(La,A)_3Mn_2O_7$ compounds are larger in magnitude than that of the $(La,A)MnO_3$.[25,30] This difference in MR is not only due to the narrowing of the one electron band width in $(La,A)_3Mn_2O_7$ but also due to the spin correlation which is inherent in the two-dimensional compounds.[31]

The magnetic-field effect on the resistivity of $(La_{1-y}Eu_y)_{1.4}Sr_{1.6}Mn_2O_7$ (shown in Fig. 7) is different from that of $La_{1.4}(Sr_{1-y}Ca_y)_{1.6}Mn_2O_7$. It is found that for Eu containing (with $y=0.1$) sample the suppression of resistivity under magnetic field is more than that of the Ca containing ($y=0.1$) sample. But for $y=0.2$ the resistivity suppression under magnetic field for Eu containing is much less than that of Ca containing sample. The MR ratio at T_{mr} for $(La_{1-y}Eu_y)_{1.4}Sr_{1.6}Mn_2O_7$ with $y=0.1$ is 90% whereas for $y=0.2$ no prominent peak is observed in the temperature variation of MR ratio data. This indicates that the substitution of Eu for La is more effective than the substitution of Ca for Sr in the lattice effects on the transport properties of

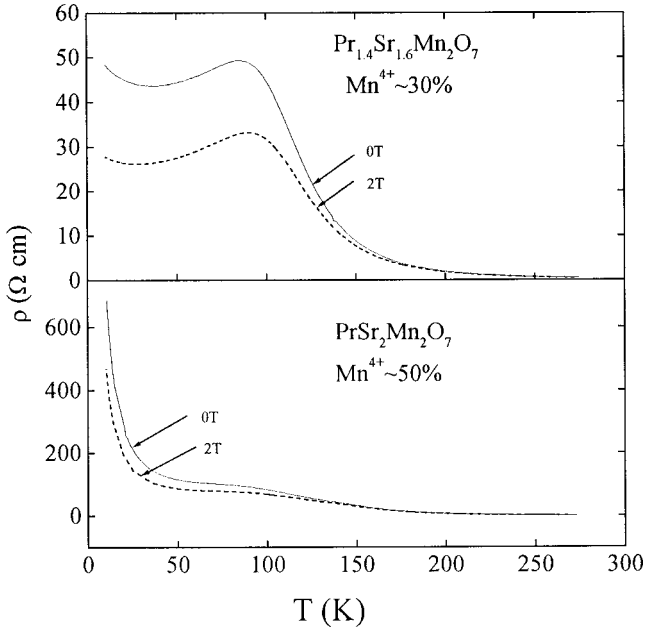

FIG. 8. Temperature variation of resistivity of $Pr_{1.4}Sr_{1.6}Mn_2O_7$ and $PrSr_2Mn_2O_7$ at 0 and 2 T magnetic fields.

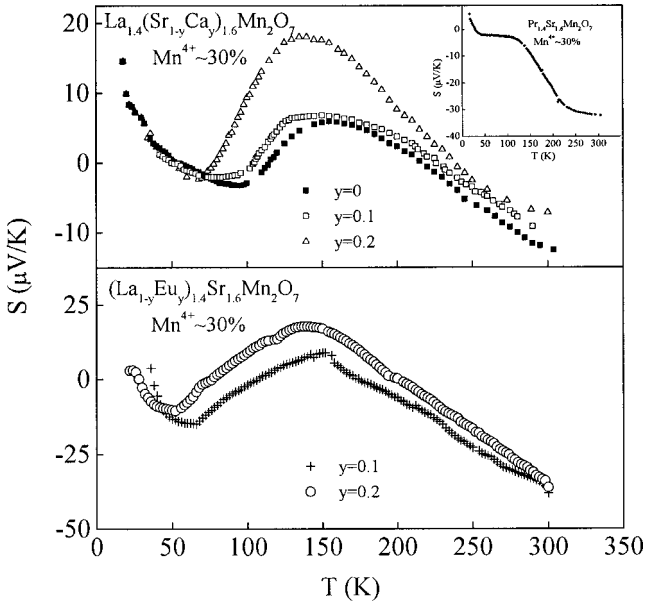

FIG. 9. Temperature variation of thermoelectric power of $La_{1.4}(Sr_{1-y}Ca_y)_{1.6}Mn_2O_7$ with $y=0$, 0.1, and 0.2 and $(La_{1-y}Eu_y)_{1.4}Sr_{1.6}Mn_2O_7$ with $y=0.1$ and 0.2. Inset: temperature variation of TEP of $Pr_{1.4}Sr_{1.6}Mn_2O_7$.

$La_{1.4}Sr_{1.6}Mn_2O_7$. It is well known that the transport properties, magnetoresistance, and magnetic transition are strongly correlated in these CMR manganese perovskites. The lattice effects (chemical pressure) induced by Eu substitution for La or Ca for Sr on the transport properties of $La_{1.4}Sr_{1.6}Mn_2O_7$ are consistent with those reported in $(La_{1-z}Nd_z)_{1.4}Sr_{1.6}Mn_2O_7$.[32] The effect of magnetic field on the resistivity of $Pr_{1.4}Sr_{1.6}Mn_2O_7$ and $PrSr_2Mn_2O_7$ are also shown in Fig. 8. It is found that the MR ratio decreases from La to Pr. We have already seen in Fig. 6 that with increasing Ca in $La_{1.4}(Sr_{1-y}Ca_y)_{1.6}Mn_2O_7$ and $La(Sr_{1-y}Ca_y)_2Mn_2O_7$, the MR ratio increases. Thus even the Mn valence level is same, the *A*-site ionic size is not an only responsible factor for the MR value. It may indicate that the MR value is also related to the magnetic interaction between *A*-site ions and Mn ions. The data described above clearly show that the transport properties of $(La, Sr)_3Mn_2O_7$ strongly depend on the electronic nature of lanthanide ions, the ionic radius of the cations, and the Mn valence level.

The temperature dependence of thermoelectric power for $La_{1.4}(Sr_{1-y}Ca_y)_{1.6}Mn_2O_7$ with $y=0$, 0.1, 0.2 is shown in Fig. 9. The high sensitivity of the TEP to the composition variation is strongly pronounced. It is found that the TEP increases with decreasing temperature and after reaching a maximum value (say at temperature T_s), the TEP value decreases and becomes to a value in the range of a few μV/K. Finally it shows a minimum value in the temperature range 50–80 K. We also notice that the T_s shifts downward systematically with increasing Ca content in a very similar manner as the T_m does. With increasing Ca content, the TEP value increases which is also in close analogy with resistivity data. The temperature variation of TEP of $(La_{1-y}Eu_y)_{1.4}Sr_{1.6}Mn_2O_7$ (shown in Fig. 9) is similar to that of $La_{1.4}(Sr_{1-y}Ca_y)_{1.6}Mn_2O_7$. The temperature variation of TEP of $Pr_{1.4}Sr_{1.6}Mn_2O_7$ is also shown in Fig. 9. In this sample, the S ($T_s<T<300$ K) value increases with decreasing temperature. Below T_s, the TEP value is nearly constant down to 50 K and below 50 K it increases. These data are similar to those obtained by Fisher *et al.*[33] in $L_{2/3}Sr_{1/3}MnO_3$ ($L=$Pr and Nd). Furthermore, the less temperature dependence of TEP in this compound below T_s might be due to the absence of bulk ferromagnetism which is consistent with that claimed by Hur *et al.* in a recent paper.[26]

It is noted that the small values of S below T_s are typical in the metallic system. It is obvious from Fig. 9 that an extraordinary thermopower develops accompanying the CMR and the $S(T)$ curve mimics the measured resistivity. Therefore the $S(T)$ data and particularly the peak at T_s are signatures of ferromagnetic-paramagnetic and metal-insulator transition. It is found that the T_s always occurs above the T_m. In fact, at T_m the TEP shows the normal-metallic-like value. In general, the feature of diffusion thermopower in the metallic region (below T_s and above the upturn) can be qualitatively understood in terms of Mott's formula for the charge contribution to the Seebeck coefficient in metals:[34]

$$S=-(\pi^2/3)(k_B^2T/e)\sigma'(E_F)/\sigma(E_F), \tag{2}$$

where e is the elementary charge, $\sigma(E_F)$ is the conductivity at Fermi level, and σ' stands for $d[\sigma(E)]/dE$. The observed decrease in $|S|$ below T_m can be explained as the increase in conductivity due to the phase transition to the FM state provided that the $\sigma'\approx$const. However, if one assumes that σ' is constant and almost isotropic electrical transport properties, i.e., $\sigma^{-1}=\rho$ then according to Mott's formula, $\Delta S/S_0 \propto \Delta\rho/\rho_0$ is expected. The plotting of $\Delta S/S_0$ vs $\Delta\rho/\rho_0$ for data points of $La_{1.4}(Sr_{1-x}Ca_x)_{1.6}Mn_2O_7$ are shown in Fig. 10. The present data obviously deviate from the theoretical prediction (linearity). In fact, the Eu containing samples also show the same deviation (not shown in figure). Therefore the assumption that σ' is constant is not justifiable. This argument supports the conclusion made by Uhlenbruck *et al.*[35]

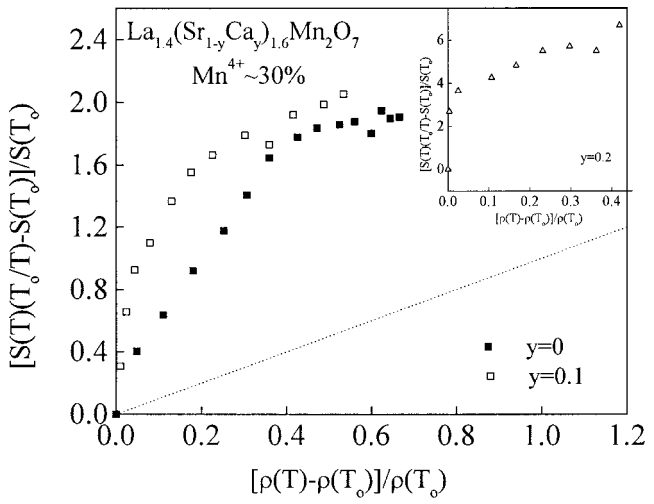

FIG. 10. Relative changes of the TEP plotted vs relative changes of the resistivity for $La_{1.4}(Sr_{1-y}Ca_y)_{1.6}Mn_2O_7$ with $y=0$ ($T_0=110$ K), $y=0.1$ ($T_0=95$ K), and $y=0.2$ ($T_0=70$ K). The dotted line represents the prediction of Mott's formula [Eq. (2)].

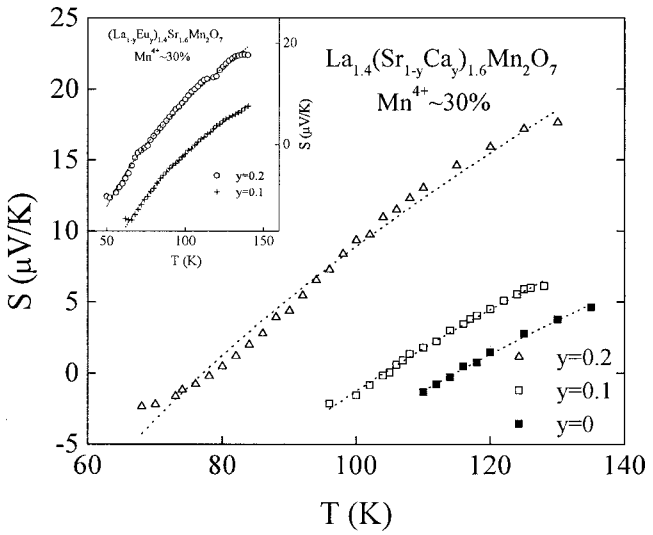

FIG. 11. Fitting of thermoelectric power data (below T_s, discussed in text) with Eq. (5) for $La_{1.4}(Sr_{1-y}Ca_y)_{1.6}Mn_2O_7$ (with $y=0$, 0.1, and 0.2) samples. Inset: Same fitting of $(La_{1-y}Eu_y)_{1.4}Sr_{1.6}Mn_2O_7$ with $y=0.1$ and 0.2.

that the assumption by Asamitsu *et al.*[36] (σ' is constant) is not valid for the moderately doped sample, such as, $La_{0.85}Sr_{0.15}MnO_3$ in the vicinity of the metal-insulator transition. Furthermore, in addition to the diffusion term, another important contribution to the TEP, namely the phonon drag effect, may be present.

Now we shall see that whether the deviation is due to the phonon drag effect. The phonon drag thermopower S_p can be expressed as[37]

$$S_p \propto 1/T. \tag{3}$$

The diffusion thermopower Eq. (2) can be simplified as

$$S_d \propto T. \tag{4}$$

Combining Eqs. (3) and (4) we obtain a simple relation valid for metal:[38]

$$S = A/T + BT. \tag{5}$$

The fitting curves for $La_{1.4}(Sr_{1-y}Ca_y)_{1.6}Mn_2O_7$ and $(La_{1-y}Eu_y)_{1.4}Sr_{1.6}Mn_2O_7$ based on Eq. (5) are shown in Fig. 11. It is seen that the experimental data can be well represented by Eq. (5) above 60 K and below T_s. Fitting parameters A and B are listed in Table II. It is found that with increasing Ca and Eu content the magnitude of the phonon drag term (A) decreases whereas that of the diffusion term (B) increases. Therefore the deviation in $\Delta S/S_0$ vs $\Delta\rho/\rho_0$ plot (Fig. 10) from the theoretical prediction is due to the presence of considerable phonon drag effect. Combining Eqs. (2) and (4), if one assumes that σ' is constant, then the ratio of B for two different samples (as for example, for $y=0.1$ and $y=0.2$) in $La_{1.4}(Sr_{1-y}Ca_y)_{1.6}Mn_2O_7$ is equal to the reciprocal ratio of the magnitude of resistivity at a fixed temperature for those two samples. The obtained $B_{y=0.1}/B_{y=0.2}$ is 0.683, whereas $\rho_{y=0.2}/\rho_{y=0.1}$ is ~6 (at $T=120$ K), i.e., both are not equal which implies that the σ' is not constant and again supports the argument mentioned above. Moreover, it is observed from previous discussion that as the TEP becomes more positive the phonon drag thermopower decreases and diffusion thermopower increases. It is known that the phonon drag effect decreases with the increase of resistivity, since the increase of resistivity means the reduction in phonon heat current and also there is a reduction in momentum transferred to the electrons, i.e., of the phonon drag effect.[39,40] This also explains that the doping in the (La, Sr) site may induce a canting of the ferromagnetic Mn spin configuration. This spin canting leads to the increase of electrical resistivity and so the S_p decreases and the S_d increases.

While describing the resistivity data in the semiconducting part, we have shown that those data can be discussed with small polaron hopping. According to the small polaron theory the thermopower can be expressed as

$$S(T) = k_B/e[E_s/k_BT + \alpha], \tag{6}$$

where E_s is the activation energy for the TEP and α is the sample dependent constant. Above T_s, the thermopower for samples studied here obeys the prediction of the small polaron theory, since S vs $1000/T$ curves fit well with straight lines (Fig. 12). From the linear fit of the curves the obtained activation energies for thermopower vary from 4 to 8 meV with the Ca content. The different values of the activation energies for the resistivity and the TEP are consistent with the conduction due to the hopping of charge carriers.

TABLE II. The best-fit parameters (A and B) obtained by fitting the metallic part of the TEP data to Eq. (5), and the T_s (the temperature where the TEP value is maximum and which varies with y in a similar manner to T_m) of $La_{1.4}(Sr_{1-y}Ca_y)_{1.6}Mn_2O_7$ and $(La_{1-y}Eu_y)_{1.4}Sr_{1.6}Mn_2O_7$.

Sample	A (μV)	B (μV/K^2)	T_s (K)
$La_{1.4}Sr_{1.6}Mn_2O_7$	−1698.3	0.129 12	154
$La_{1.4}(Sr_{0.9}Ca_{0.1})_{1.6}Mn_2O_7$	−1625.9	0.150 21	146
$La_{1.4}(Sr_{0.8}Ca_{0.2})_{1.6}Mn_2O_7$	−1306.2	0.219 92	136
$(La_{0.9}Eu_{0.1})_{1.4}Sr_{1.6}Mn_2O_7$	−1521.8	0.133 06	140
$(La_{0.8}Eu_{0.2})_{1.4}Sr_{1.6}Mn_2O_7$	−1306.2	0.200 03	150

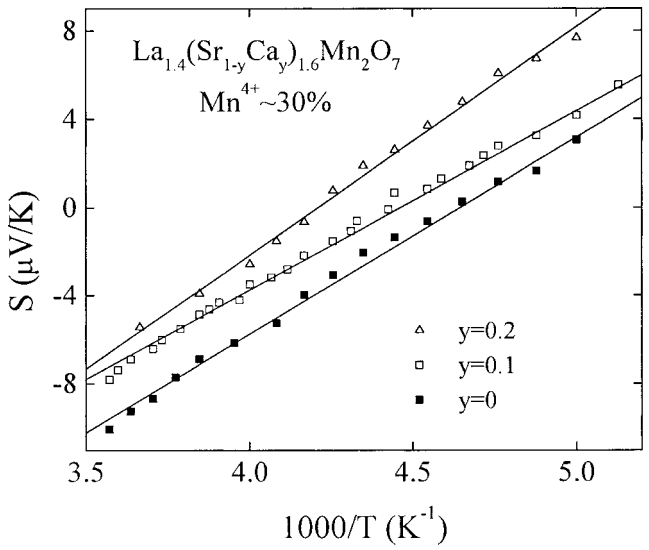

FIG. 12. Thermoelectric power vs $1000/T$ for $La_{1.4}(Sr_{1-y}Ca_y)_{1.6}Mn_2O_7$ with $y=0$, 0.1, and 0.2 (above T_s, discussed in text).

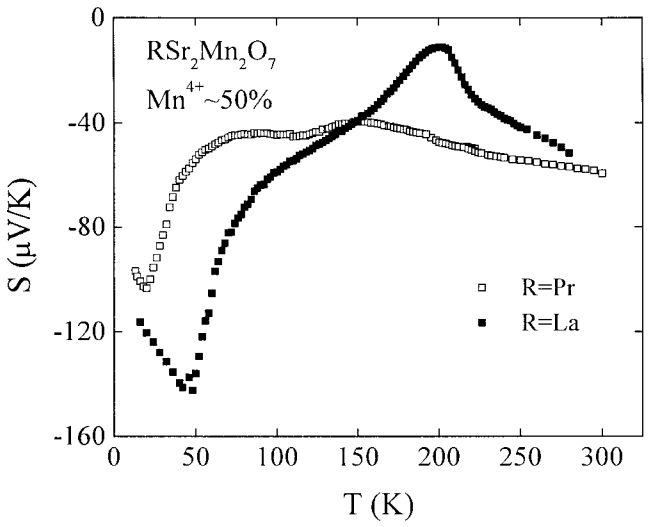

FIG. 13. Temperature variation of thermoelectric power of $RSr_2Mn_2O_7$ (R=La and Pr).

The $S(T)$ data for $RSr_2Mn_2O_7$ (R=La, Pr) shown in Fig. 13 are more negative than those of $R_{1.4}Sr_{1.6}Mn_2O_7$. Below T_s the TEP behavior is a little complicated. Here, the T_s is higher than the T_m in $RSr_2Mn_2O_7$ which is similar to that in $R_{1.4}Sr_{1.6}Mn_2O_7$. In view of the results found in $R_{1-x}A_xMnO_3$-type oxides, the doping ratio in $R_{1.4}(Sr_{1-y}Ca_y)_{1.6}Mn_2O_7$, where Mn^{4+} is 30%, seems very close to optimal value (i.e., $x \sim x_c$) to exhibit the CMR characteristics.[41,42] Therefore in $RSr_2Mn_2O_7$, where Mn^{4+} is 50%, the doping level is $x > x_c$. The more negative value of TEP for $RSr_2Mn_2O_7$ might be due to the fact that for $x > x_c$ the hopping barrier decreases with increasing energy, so the contribution to the thermopower from the energy dependence of the hopping barrier is negative.[43] Furthermore, the complicated T dependence of S in the low-temperature regime is similar to that observed in the doped La_2CuO_4 and most likely is related to the charge ordering phenomena.[35] The different values of T_m and T_s may be due to the different temperature dependencies of thermopower and resistivity.[44] We also tried to fit the TEP data of $RSr_2Mn_2O_7$ below T_s to Eq. (5). But the experimental data cannot be well fitted with the theoretical curve. This might be also due to the presence of charge ordering. The activation energies (E_ρ and E_s) calculated respectively from $\ln(\rho)$ vs $1000/T$ and S vs $1000/T$ plots (not shown), similar to $La_{1.4}(Sr_{1-y}Ca_y)_{1.6}Mn_2O_7$ system, differ from each other. Therefore we may conclude that the charge transport occurs due to the hopping of carriers rather than a semiconducting-like activated conduction. Furthermore, for each compound, the value of S tends to fluctuate due to a rather small conductivity at low temperatures. Since both the diffusion and hopping (if present) terms approach zero as $T \to 0$,[45] the rapid increase in S (below 50–80 K) may not be explained unless it has a large contribution from the phonon drag effect.

IV. CONCLUSION

We have investigated the lattice effects on the transport properties of $(R,Sr)_3Mn_2O_7$ by studying the resistivity, MR, and TEP. In $La_{1.4}(Sr_{1-y}Ca_y)_{1.6}MnO_7$ above T_m the conduction behavior is due to the small polaron hopping. A changeover from the adiabatic to the nonadiabatic regime in the hopping mechanism is observed when Mn^{4+} concentration changes from 30 to 50 %. The maximum MR value is found in $La_{1.4}(Sr_{1-y}Ca_y)_{1.6}Mn_2O_7$ for $y=0.2$ which might be due to the defects in La sites as well as in oxygen sites in the compound. The MR data in $La(Sr_{1-y}Ca_y)_2Mn_2O_7$ do not show any peak value which is in contrast with that in $La_{1.4}(Sr_{1-y}Ca_y)_{1.6}Mn_2O_7$. This might be due to the presence of a more complex magnetic interaction dominated by superexchange over double exchange. The possible charge ordering of Mn^{3+} and Mn^{4+} in $RSr_2Mn_2O_7$ could also lead to the electron localization and contribute to the complex nature of this transition. The MR value decreases when R goes from La to Pr. But the MR increases when the Ca and Eu content increase. Therefore the MR depends not only on A-site ionic size but also the magnetic interaction between lanthanides and Mn ions. Both the resistivity and TEP data in $RSr_2Mn_2O_7$ indicate the charge ordering at lower temperature. In $RSr_2Mn_2O_7$, the TEP is more negative than that of $R_{1.4}Sr_{1.6}Mn_2O_7$, which is due to the fact that for the doping level more than optimal, the hopping barrier decreases with increasing energy. Hence the contribution to the S from the energy dependence of the hopping barrier is negative. The low-temperature upturn in TEP behavior of all the samples may be due to the phonon drag effect.

ACKNOWLEDGMENT

This work was supported by National Science Council of Republic of China under Contract No. NSC89-2112-M110-008.

[1] G. H. Jonker, Physica (Amsterdam) **22**, 707 (1956).
[2] R. von Helmholt, J. Wecker, B. Holzapfel, M. Schultz, and K. Samwer, Phys. Rev. Lett. **71**, 2331 (1989).
[3] K. Chahara, T. Ohno, M. Kasai, and Y. Kozono, Appl. Phys. Lett. **63**, 1990 (1993).
[4] S. Jin, T. H. Tiefel, M. McCormack, R. A. Fastnacht, R. Ramesh, and L. H. Chen, Science **264**, 413 (1994).
[5] Y. Tomioka, A. Asamitsu, Y. Moritomo, H. Kuwahara, and Y. Tokura, Phys. Rev. Lett. **74**, 5108 (1995).
[6] H. Kuwahara, Y. Tomioka, A. Asamitsu, Y. Moritomo, and Y. Tokura, Science **270**, 961 (1995).
[7] P. Schiffer, A. P. Ramirez, W. Bao, and S-W. Cheong, Phys. Rev. Lett. **75**, 3336 (1995).
[8] J. M. D. Coey, M. Viret, L. Ranno, and K. Ounadjela, Phys. Rev. Lett. **75**, 3910 (1995).
[9] P. G. Radaelli, D. E. Cox, M. Marezio, and S.-W. Cheong, Phys. Rev. B **55**, 3015 (1997).
[10] A. Asamitsu, Y. Moritomo, Y. Tomioka, T. Arima, and Y. Tokura, Nature (London) **373**, 407 (1995).
[11] Y. Shimakawa, Y. Kubo, and T. Manako, Nature (London) **379**, 53 (1996).
[12] S.-W. Cheong, H. Y. Hwang, B. Batlogg, and L. W. Rupp, Solid State Commun. **98**, 163 (1996).
[13] P. D. Battle, S. J. Blundell, M. A. Green, W. Hayes, M. Honold, A. K. Klehe, N. S. Laskey, J. E. Mollburn, L. Murphy, M. J. Rossrinsky, N. A. Samarin, J. Singleton, N. E. Sluchanko, S. P. Sullivan, and J. F. Vente, J. Phys.: Condens. Matter **8**, L427 (1996).
[14] Y. Moritomo, A. Asamitsu, H. Kuwahara, and Y. Tokura, Nature (London) **380**, 141 (1996).
[15] S. N. Ruddlesden and P. Popper, Acta Crystallogr. **11**, 54 (1958).
[16] D. N. Argyriou, J. F. Mitchell, J. B. Goodenough, O. Chmaissem, S. Short, and J. D. Jorgensen, Phys. Rev. Lett. **78**, 1568 (1997).
[17] C. F. Chang, P. H. Chou, H. L. Tsay, S. S. Weng, S. Chatterjee, H. D. Yang, R. S. Liu, C. H. Shen, and W.-H. Li, Phys. Rev. B **58**, 12 224 (1998).
[18] J. L. García-Munõz, J. Fontcuberta, B. Martinez, A. Seffar, S. Piñol, and X. Obradors, Phys. Rev. B **55**, R668 (1997).
[19] J. L. García-Munõz, J. Fontcuberta, M. Suaaidi, and X. Obradors, J. Phys.: Condens. Matter **8**, L787 (1996).
[20] P. G. Radaelli, G. Iannone, M. Marezio, H. Y. Hwang, S.-W. Cheong, J. D. Jorgensen, and D. N. Argyriou, Phys. Rev. B **56**, 8265 (1997).
[21] N. F. Mott, J. Non-Cryst. Solids **1**, 1 (1968); E. A. Davis and N. F. Mott, Philos. Mag. **22**, 903 (1970).
[22] M. Sayer and A. Mansingh, Phys. Rev. B **6**, 4629 (1972).
[23] D. C. Worledge, G. Jeffrey Snyder, M. R. Beasley, T. H. Geballe, R. Hiskes, and S. DiCarolis, J. Appl. Phys. **80**, 5158 (1996).
[24] H. Y. Hwang, T. T. M. Palstra, S.-W. Cheong, and B. Batlogg, Phys. Rev. B **52**, 15 046 (1995).
[25] A. Urushibara, Y. Moritomo, T. Arima, A. Asamitsu, G. Kido, and Y. Tokura, Phys. Rev. B **51**, 14 103 (1995).
[26] N. H. Hur, J.-T. Kim, K. H. Yoo, Y. K. Park, J.-C. Park, E. O. Chi, and Y. U. Kwon, Phys. Rev. B **57**, 10 740 (1998).
[27] D. N. Argyriou, J. F. Mitchell, P. G. Radaelli, H. N. Bordallo, D. E. Cox, M. Medarde, and J. D. Jorgensen, Phys. Rev. B **59**, 8695 (1999).
[28] M. Medarde, J. F. Mitchell, J. E. Millburn, S. Short, and J. D. Jorgensen, Phys. Rev. Lett. **83**, 1223 (1999).
[29] R. Mahesh, R. Wang, and M. Itoh, Phys. Rev. B **57**, 104 (1998).
[30] R. Mahesh, R. Mahendran, A. K. Raychaudhuri, and C. N. R. Rao, J. Solid State Chem. **122**, 448 (1996).
[31] H. Asano, J. Hayakawa, and M. Mitsui, Phys. Rev. B **57**, 1052 (1998).
[32] Y. Moritomo and M. Itoh, Phys. Rev. B **59**, 8789 (1999).
[33] B. Fisher, L. Patlagan, and G. M. Reisner, Phys. Rev. B **54**, 9359 (1996).
[34] M. Cutler and N. F. Mott, Phys. Rev. **181**, 1336 (1969).
[35] S. Uhlenbruck, B. Buchner, R. Gross, A. Freimuth, A. Maria de Leon Guevara, and A. Revcolevschi, Phys. Rev. B **57**, R5571 (1998).
[36] A. Asamitsu, Y. Moritomo, and Y. Tokura, Phys. Rev. B **53**, R2952 (1996).
[37] R. D. Barnard, *Thermoelectricity in Metals and Alloys* (Taylor & Francis, London, 1972).
[38] J. L. Cohn, S. A. Wolf, V. Selvamanickam, and K. Salama, Phys. Rev. Lett. **66**, 1098 (1991).
[39] A. B. Kaiser, Phys. Rev. B **35**, 4677 (1987).
[40] S. Chatterjee, S. Banerjee, B. K. Chaudhuri, N. Froumin, M. Polak, and J. Baram, Phys. Rev. B **54**, 10 143 (1996).
[41] Y. Tokura, Y. Tomioka, H. Kuwahara, A. Asamitsu, Y. Moritomo, and M. Kasai, J. Appl. Phys. **79**, 5288 (1996).
[42] C. N. R. Rao, A. K. Cheetham, and R. Mahesh, Chem. Mater. **8**, 2421 (1996).
[43] V. H. Crespi, L. Lu, Y. X. Jia, K. Khazeni, A. Zettl, and M. L. Cohen, Phys. Rev. B **53**, 14 303 (1996).
[44] J. Fontcuberta, A. Seffar, X. Granados, García-Munõz, X. Obradors, and S. Piñol, Appl. Phys. Lett. **68**, 2288 (1996).
[45] B. Movaghar and W. Schirmacher, J. Phys. C **14**, 859 (1981).